DIFFERENCES IN SYNCHROTRON RADIATION INDUCED GAS DESORPTION FROM STAINLESS STEEL AND ALUMINIUM ALLOY

M. Andritschky, O. Gröbner, A.G. Mathewson, P. Strubin
CERN, Geneva, Switzerland
R. Souchet, LURE, Orsay, France
B. Trickett, ESRF, Grenoble, France

A comparative study has been made of the synchrotron radiation induced gas desorption from vacuum chambers made of stainless steel and aluminium alloy. The sample vacuum chambers of about 3.6 m length have been exposed to synchrotron radiation on an external photon beam line at the DCI storage ring in Orsay. The desorbed gas species are H_2, CH_4, CO and CO_2. The gradual decrease of the desorption yield with continued exposure to radiation - the dynamic cleaning effect - and the influence of a high temperature thermal treatment of the stainless steel vacuum chamber on the desorption process have been investigated. The different behaviour of the aluminium and the stainless steel - for the latter both a lower level of gas desorption and a lower cleaning rate are found - is interpreted in terms of the photoelectron production and the different surface oxide layers.

1. Introduction

Synchrotron radiation induced neutral gas desorption (SRD) due to circulating highly relativistic electrons or positrons is responsible for most of the gas load in storage rings. This paper presents a comparative study of the synchrotron radiation induced gas desorption from aluminium and stainless steel. 3.6 m long vacuum chambers, made of the extruded aluminium profile used in LEP and of 316 LN stainless steel were tested at glancing angle of photon incidence at DCI. The critical energy of the photon beam was varied between 0.77 and 3.5 keV by operating the DCI storage ring at different beam energies. Since the gas desorption is caused by both, incident photons and by photoelectrons, the measurements were complemented by electron stimulated desorption (ESD) experiments for the two considered materials.

2. Experimental set-up

Two, in principle similar, experimental set-ups were used for the photon and electron stimulated desorption experiments. The experimental facility used for the SRD experiments, which is described in detail elsewhere [1], consists essentially of the 3.6 m long vacuum test chamber, equipped with a quadrupole residual gas analyser, a total pressure gauge and a pumping system consisting of a combination of an ion pump and a Ti sublimation pump. At an angle of 11 mrad between test chamber and the photon beam (this configuration was maintained constant throughout the experiments), the chamber was exposed to the synchrotron radiation over 3.12 m. In a second laboratory set-up, electron stimulated neutral gas desorption was measured by accelerating electrons from a hot tungsten filament, biased negatively and positioned in the centre of the vessel, towards the test chamber wall. Boths test systems, SRD-and ESD, were pumped through an orifice with a known conductance. Desorption yields were obtained from the specific pressure rise p_i and the specific conductance S_i of the orifice which represents the pumping speed for the test system.

3. Molecular desorption yield and accumulated number of photons

The total incident photon flux N_p per metre of test chamber depends on the electron beam energy E_e, the electron beam current I_e and is determined by the collimation of the photon beam. In our configuration we have

$$N_p = 1.93\ 10^{14}\ E_e\ I_e \quad \text{photons/s m} \qquad (1)$$

The accumulated number of photons, the photon dose D, is simply the integral of N_p over time t

$$D = \int_0 N_p dt \qquad (2)$$

To convert the photon dose per metre into photons per square centimetre, the perimeter of the test chambers, 36 cm for the aluminium chamber and 43 cm for the stainless steel chamber, has been used. This assumes that the desorption by primary photons and by scattered photons is equal.

The specific desorption yield η_i for the main desorbed gases is calculated from the specific pressure rise p_i [mbar], the specific pumping speed S_i [l/s] and the incident flux of photons or electrons respectively.

$$\eta_{i,p} = 8.67\ 10^{19} \frac{p_i\ S_i}{N_p} \quad \text{mol/photon}$$

$$\eta_{i,e} = 2.72\ 10^{19} \frac{p_i\ S_i}{N_e} \quad \text{mol/electron} \qquad (3)$$

The SRD test system also permitted the measurement of the photoelectron production using a wire electrode with an effective length of 33 cm positioned in the centre of the test chamber and biased positively to 1000 V. The photoelectron yield ρ is derived from the collected current I_e [A] on this wire.

$$\rho = 5.57\ 10^{19} \frac{I_e}{N_p} \qquad (4)$$

4. Material treatment

The two materials studied were aluminium type ISO AlMgSi and stainless steel type 316 LN. The stainless steel vessels were made out of hot-rolled, work-hardened sheet metal. The aluminium test chamber and the stainless steel vessels were cleaned according to a procedure consisting of the following steps :

- Immersion in perchlorethylene vapour at 121°C
- Ultrasonic cleaning in alcaline detergent at 65°C
- Immediate rinsing in demineralized water
- Drying in a hot air oven at 150°C
- Vacuum bakeout at 150°C (aluminium) and 300°C (stainless steel)
- Second bakeout at 150°C after installation in the experimental facility.

In addition, the second stainless steel vessel was given a special high temperature treatment at 950 °C under vacuum between the chemical cleaning and before the 300 °C bakeout. After the chemical cleaning, the metal surfaces are covered by their omnipresent oxide layer i.e. about 35 Å of aliminium hydroxide on the aluminium alloy and 25 Å of (Fe,Ni,Cr)-oxide on stainless steel. On both materials, a carbon contamination of about 20% could be measured by Auger analysis made 'in situ' after bakeout. The topography of the surfaces, as seen by the scanning electron microscope, for the two materials after this treatment is found to be significantly different (see Fig. 1). The surface roughness factor, expressing the ratio between real and geometric surface and hence affecting the amount of surface gas, was estimated for aluminium in the range from 2 to 4 [3] and for stainless steel at about 14 [4].

CH2669-0/89/0000-0563$01.00©1989 IEEE

a b

Fig.1 Surface of (a) stainless steel [2] and (b) aluminium as seen by the scanning electron microscope (x3000, viewing angle 45°). The bar represents 4 μm.

5. Experimental results and discussion

5.1 Photoelectron yield

Synchrotron radiation photons may desorb gas molecules either directly or, more efficiently, indirectly by the resulting photoelectrons. To estimate the contribution of the photoelectrons on the neutral gas desorption, the photoelectron yield ρ was measured for aluminium and stainless steel at normal and at gracing angle of photon incidence. The results are shown in Fig.2.

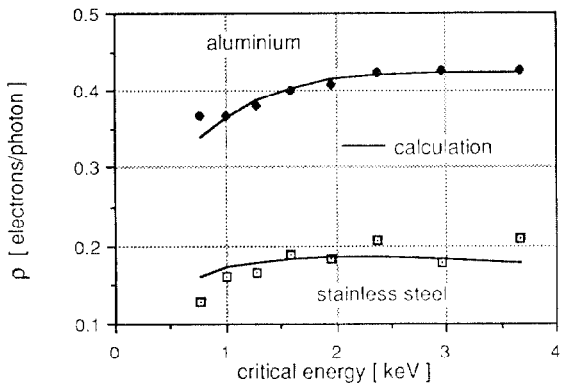

Fig.2 Photoelectron yield ρ at 11 mrad incidence of the synchrotron radiation for aluminium and stainless steel. The solid curves are calculated from eq.5. Note that the calculated values for stainless steel have been devided by a factor of 5 to fit the experimental points.

The photoelectron production ρ for aluminium may be calculated with good agreement using the photoelectron yield Y (E) at normal photon incidence and the photon reflectivity R(E) scaled to the angle ß between the photon beam and the surface. We find that the calculated photoelectron production on stainless steel agrees much less with the experiment, probably because the data for Y(E) and R(E) were not available and instead data for nickel had to be used [6,7].

$$\rho = \int_{5eV}^{\infty} Y(E)\ (1-R(E))\ \frac{1}{\sin ß}\ N_p(E)\ dE \qquad (5)$$

The result of calculations according to eq.5, which has been described in detail in ref. [5], is included in Fig.2.

5.2 Molecular desorption yield

The molecular desorption yield η_i for the main desorbed gases H_2, CH_4, CO and CO_2 at the beginning of the experiment is listed in table1 for the ESD and SRD experiments from aluminium and from stainless steel. The desorption yield from stainless steel with and without a 950 °C high temperature treatment was found to be the same within the experimental uncertainties.

	Aluminium		Stainless Steel	
	$\eta_{i,e}$	$\eta_{i,p}$	$\eta_{i,e}$	$\eta_{i,p}$
$\eta\ H_2$	0.57	0.2-0.5	$2.7\ 10^{-2}$	$1.3\ 10^{-3}$
$\eta\ CH_4$	$1.2\ 10^{-2}$	$2.5\ 10^{-3}$	$1.3\ 10^{-3}$	$4.8\ 10^{-3}$
$\eta\ CO$	$5.8\ 10^{-2}$	$3.6\ 10^{-2}$	$3.3\ 10^{-3}$	$2.5\ 10^{-4}$
$\eta\ CO_2$	$8.3\ 10^{-2}$	$3.4\ 10^{-2}$	$4.3\ 10^{-3}$	$3.5\ 10^{-4}$

Table 1: Molecular desorption yield η_i for aluminium and stainless steel exposed to synchrotron radiation with a critical energy of 2.95 keV and 11 mrad photon incidence and to electrons with an energy of 150-300 eV.

Using this table and the values in figure 2, we find that for aluminium the PSD desorption yield $\eta_{i,p}$ may be calculated using the ESD desorption yield $\eta_{i,e}$ and the photoelectron production ρ . Thus neglecting direct photodesorption we may use

$$\eta_{i,p} = \rho\ \eta_{i,e} \qquad (6)$$

For stainless steel the same calculation for SRD gives values slightly higher than the ones measured. This would suggest, that the mean photoelectron energy and, hence also the ESD gas desorption yield for stainless steel, are lower than for aluminium.

The molecular desorption yield of the gases H_2, CH_4, CO and CO_2 is shown in figure 3 as a function of the critical energy of the photon spectrum.

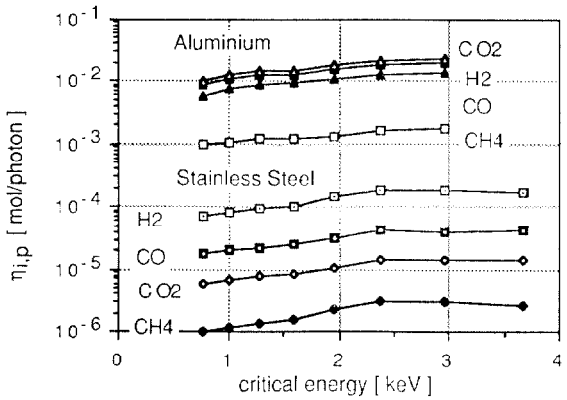

Fig.3 The dependence of the measured molecular desorption yield η on the critical photon beam energy for aluminium and stainless steel with 11 mrad photon incidence. Prior to this measurement, the chambers had been exposed to a dose D ≈1.2 10^{21} photons/m and D ≈ 2.4 10^{21} photons/m for the aluminium and the stainless steel chamber, respectively.

5.3 Beam cleaning

During continuous photon or electron exposure the gas desorption decreases due to the cleaning of the surface. Figures 4 and 5 show the desorption yield as a function of the photon dose. More than 2 10^{21} photons/m were accumulated during each run. The photon beam critical energy was 2.95 keV and the angle of incidence 11 mrad. Arrows in the figures indicate an increasing photon intensity from 6.65 10^{14} to 1.66 10^{16} and finally to 8.3 10^{16} photons/s m. This change of radiation intensity coincides with discontinuities of the desorption yield. For H_2 and CO the

desorption decreases with time t as $t^{-1/2}$. A model describing the clean-up of the surface as a process where the time dependance is determined by gas transport via diffusion in the surface oxide layer [3,8,9] has been applied to our data and the result is represented by the solid lines in Fig4 and Fig5. This diffusion model describes both the hydrogen desorption yield decreasing with time and the discontinuities of the desorption yield when the intensity is increased. For the calculations a diffusion coefficient of approx. $2\ 10^{-19}$ cm^2/s was used for both, aluminium and stainless steel. The model is restricted to the behaviour of hydrogen, because for H_2, the effect of chemical reactions may be neglected. However, CO shows a similar behaviour to H_2 thus the proposed model may also be applicable for CO.

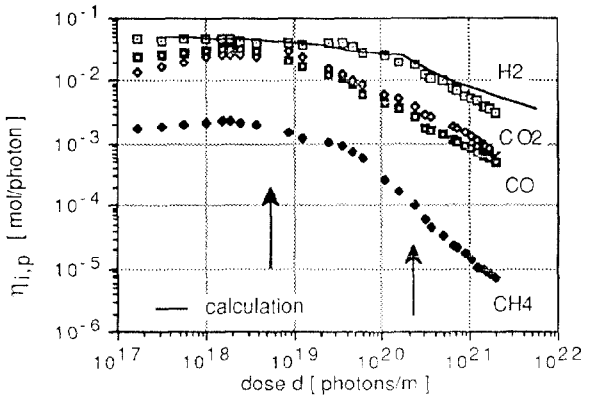

Fig.4 The molecular desorption yield $\eta_{i,p}$ for the gases H_2, CH_4, CO and CO_2 as a function of the accumulated photon dose for aluminium.

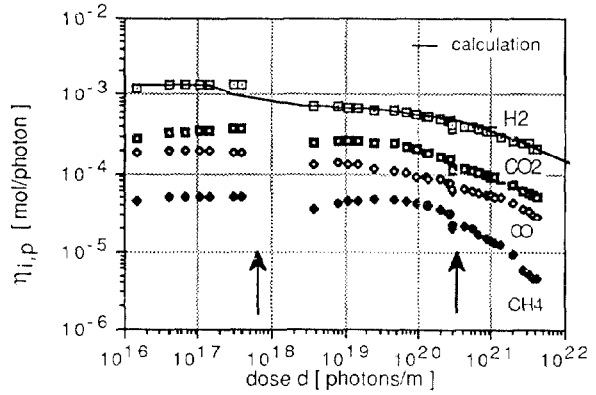

Fig.5 The molecular desorption yield $\eta_{i,p}$ for the gases H_2, CH_4, CO and CO_2 as a function of the accumulated photon dose for stainless steel.

6. Comparison between Aluminium and Stainless steel

The initial molecular gas desorption yield for aluminium and stainless steel can be described by the photoelectron production and by the ESD of these photoelectrons. For both materials the photon stimulated desorption appears to be negligible. The synchrotron radiation induced initial gas desorption yield of stainless steel chambers is about 50-150 times lower than for aluminium. This may be partly a consequence of the lower photoelectron production and partly of the smaller mean energy of the photoelectrons for stainless steel. Alternatively, it is not established whether the lower gas desorption yield for photoelectrons is due to a 'by nature' more stable oxide layer on the stainless steel alloy or due to the slightly different material treatment. The 300°C bakeout of the stainless steel test chambers - in comparison with the 150°C bakeout of the aluminium tube - may also influence the gas desorption yield. However, this would be in contradiction with our finding that the 950°C high temperature treatment of stainless steel didnot provide a lower desorption yield once installed on the test system.

The lower beam cleaning rate of stainless steel in comparison with aluminium may be attributed to the larger real surface area. Due to this larger surface, the specific radiation intensity is reduced and at the same time also the desorption rate per square centimetre.

Acknowledgements

We are indebted to Dr. P. Marin for his continued interest in this work and for the many fruitful and critical discussions on this subject. We would also like to thank W. Unterlerchner for providing the scanning electron microscope pictures of our samples.

References

[1] O. Gröbner, A. G. Mathewson, H. Störi, P. Strubin and R. Souchet, Vacuum, 33, pp.397 (1983)

[2] W. Unterlerchner, private communication, internal note CERN-ISR-VA/77-7

[3] M. Andritschky to be published in Vacuum, (1989)

[4] K. Watanabe, S. Maeda, T. Yamashina and A. G. Mathewson, J. Nucl. Mater. 93/94, pp.679, (1980)

[5] O. Gröbner, A. G. Mathewson, P. Strubin, E. Alge, to be published in J. Vac. Sci. Technol.

[6] R. H. Day J. Appl. Physics, 52 (11), pp.6965, (1981)

[7] H. J. Hagemann, Hamburg, DESY report, DESY SR-74/7, May (1974)

[8] M. Andritschky, O. Gröbner, A. G. Mathewson, F. Schumann, P. Strubin and R. Souchet, Vacuum, 38, pp.933, (1988)

[9] K. Dimoff and Ashok K. Vijh, Surface Technol., 25, pp.175, (1985)